CrossMark

Effect of Potassium on the Physiochemical and Catalytic Characteristics of V_2O_5/TiO_2 Catalysts in *o*-Xylene Partial Oxidation to Phthalic Anhydride

Philipp Eversfield[1] · Wenjing Liu[1] · Elias Klemm[1]

Abstract

Abstract   Vanadia species formed on the surface depend on the K/V atomic ratio. At small K/V ratios, Raman spectra show the formation of the K-doped and K-perturbed monomeric species. At K/V = 1, kristalline KVO_3 is mainly present on the surface. In situ high temperature XRD-results exhibit a promoting effect on the anatase to rutile phase transformation in the presence of 0.03 and 0.21 wt% potassium. Large amount of K (3 wt%) provides thermal stability of V/Ti/O catalyst and no transformation is found up to 600 °C. Reduction of vanadia K-doped vanadia catalysts is moved to higher temperatures than for the catalyst without potassium. The catalyst having 0.21 wt% K possesses the highest activity in *o*-xylene oxidation. Furthermore, the K-doped monomeric vanadia species in this catalyst leads to a promoted adsorption or a prevented desorption of phthalide, resulting in a decreased selectivity towards phthalide and CO_x and a increased PA selecticity.

Graphical Abstract
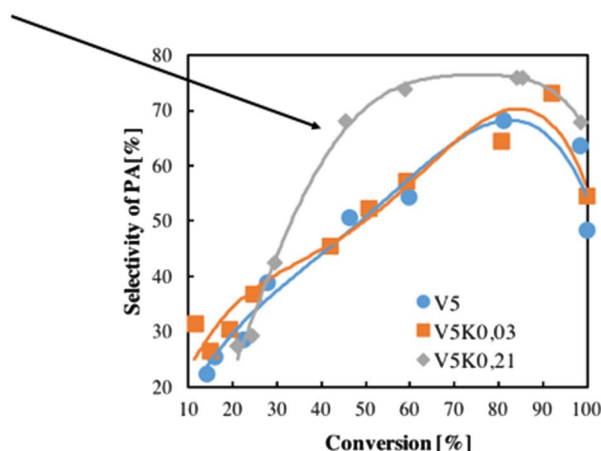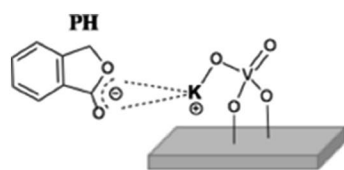
✉ Philipp Eversfield
    philipp.eversfield@itc.uni-stuttgart.de

✉ Elias Klemm
    elias.klemm@itc.uni-stuttgart.de

[1] Faculty of Chemistry, Institute of Chemical Technology, University of Stuttgart, Pfaffenwaldring 55, 70569 Stuttgart, Germany

Springer

1 Introduction

As a versatile intermediate in organic chemistry, phthalic
anhydride (PA) is mainly used in the manufacture of phtha-
late plasticizers for PVC, alkyl resins, phthalocyanines
and polyesters [1]. Modern, commercial processes for the
production of phthalic anhydride are based on the het-
erogeneously catalyzed gas phase oxidation of *o*-xylene
over a multi-layer catalytic fixed-bed containing V$_2$O$_5$/
TiO$_2$ catalysts at a temperature between 350 and 390 °C
[2–4]. Besides the target product PA, *o*-Tolualdehyde
(TA), phthalide (PH) and carbon oxides (CO$_2$ and CO)
are formed. Numerous investigations have been devoted
to kinetic studies and reaction mechanisms, however, due
to the complicity of the catalytic system, there are always
some contradictory views. In many publications, a reaction
network for the formation of PA was suggested as shown in
Fig. 1[5–10].

Compared with other catalysts, V$_2$O$_5$ supported on
TiO$_2$ (anatase) exhibits excellent catalytic performance
in the selective oxidation of o-xylene. A large number
of papers were published on the structure and the physi-
ochemical properties of V$_2$O$_5$/TiO$_2$ catalysts. The results
of these studies indicate that chemical interaction between
phases of V$_2$O$_5$ and TiO$_2$ leads to the formation of a two-
dimensional vanadia layer [11, 12], which is considered
as the active phase in selective catalytic oxidation and
shows a higher activity and selectivity than bulk V$_2$O$_5$
crystallites [13]. In unhydrated conditions, this layer con-
sists of isolated surface monomeric species and polymeric

(metavanadate-like) species with tetrahedrally coordinated
vanadium [14, 15].

It was mentioned that the presence of impurities in com-
mercial support titania such as phosphorus [11, 12] and
potassium [16, 17] may significantly influence the catalytic
behavior. This means that a noticable modification on both,
activity and selectivity to phthalic anhydride can be real-
ized with the selective addition of promoters. Despite the
well-known importance of promoters, there are only few
publications dealing with the catalytic properties of doped
V/Ti/O catalysts. As one of the main impurities, potas-
sium affects the length of V=O bond, leading to structural
changes of monolayer catalysts [20].

In the work at hand, we investigate the structure and
physiochemical properties of undoped and K-doped V/Ti/O
systems containing different loadings of potassium. The
second part is aimed at the study of catalytic performance
in partial oxidation of *o*-xylene. The catalysts were pre-
pared from pure starting materials without mentionsworthy
impurities and vanadium loading was fixed at 5 wt% V.

2 Experimental

2.1 Catalyst Preparation

V/Ti/O catalysts were prepared via grafting [17] by add-
ing a solution of vanadyl chloride (99%, Sigma-Aldrich)
in dry toluene to hydrated titanium dioxide at 75 °C
and stirred for 5 h. The TiO$_2$ used (99.9%, Alfa Aesar)
is specified as having a surface area of 49.8 m^{2}g^{-1} and
consists predominantly of anatase. The precipitate was
rinsed with toluene and dried at 100 °C for 1 h. The
powder was moistened with a few drops of water, again
dried at 110 °C for 18 h and calcined at 400 °C for 6 h.

Fig. 1 Xxx
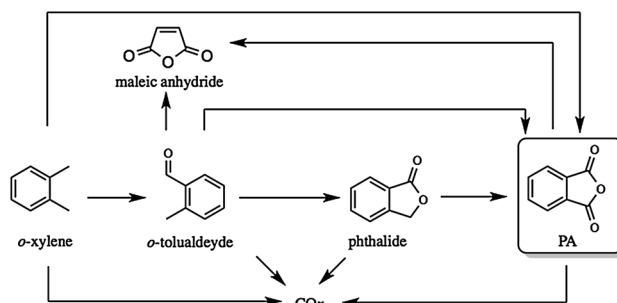
K-doped V/Ti/O catalysts with a variable amount of potassium were prepared based on the undoped V/Ti/O catalyst via wet impregnation, using an aqueous solution of potassium acetate (99%, Sigma-Aldrich). Desired amounts of promoter precursors potassium acetate were dissolved separately in distilled water under stirring and then added to the catalyst. The sample was mixed, dried for 14 h at 120 °C and subsequently calcined at 450 °C for 3 h. The catalyst without potassium addition is referred to as V5. K-doped catalysts are abbreviated as V5K*x*, where *x* is the loading of potassium on the catalysts in weight percent. Characteristics of the catalysts are listed in Table 1.

2.2 Catalyst Characterization

BET surface area of the catalysts were measured using N$_2$ adsorption–desorption at the temperature of liquid N$_2$ (77 K) by an Autosorb-3B (Quantachrome). X-ray diffraction patterns were recorded using a AXS D8 Advance diffractometer (Bruker), with Cu-K$_\alpha$ (λ=0,154 nm) as a radiation source in the range of 10°–80°, with a scanning step of 0.0165° at a counting time of 0.2 s per step. In order to investigate the phase transition of the catalysts, in situ high-temperature XRD data were obtained with a Siemens D5000 powder X-ray diffractometer, equipped with a Cu-K$_\alpha$ radiation (λ=0,154 nm), a Bragg–Brentano goniometer, and a DHRS1 custom high temperature stage. The in situ measurements were carried out in step mode between 20° and 35° with a step size of 0.01° at a counting time of 2.5 s per step. Data was collected at 40, 500 °C, and then at intervals of 10 °C, up to 600 °C. Each temperature was held for 3 h while three measurements were carried out. Raman spectroscopy experiments were performed by a Ventana 785 Raman spectrometer (Ocean optics), equipped with a Hamamatsu detector and IPS 785 nm spectrum stabilized laser Class 3B, operating at 785 nm with a varying power in the range of 50–350 mW.

Temperature programmed reduction measurements were performed using a Autosorb iQ (Quantachrome) instrument. Calcined samples, with particle sizes between 200 μm and 315 μm, were loaded in a quartz reactor and pre-treated in oxidative atmosphere (9 vol% O$_2$, rest He, flow rate: 27.5 cm^3/min) at 390 °C for 1 h. After cooling to 200 °C, the reactor was heated in a flow of 8 vol% of H$_2$ in Argon (flow rate: 26 cm^3/min) with a heating rate of 15 °C/min to 700 °C. The flow of gas mixture was maintained at 700 °C for 20 min.

2.3 Catalytic Measurements

The catalytic study was carried out using a laboratory conventional flow, fixed-bed reactor at atmospheric pressure. The feed composition (1.5 vol% *o*-xylene in air flow) was obtained by passing air through saturators filled with o-xylene. The catalyst with particle size from 200 to 315 μm was diluted with silicon carbide in a 1:40 weight ratio to avoid adverse thermal effects. Each catalyst bed had an approximate volume of 0.5 ml in a reactor with a diameter of 7.95 mm. The temperature for the catalytic measurements was set at 350 °C and monitored by a thermocouple inside the packed bed. The space velocity was varied between 0 and 3.5 L g×min with catalyst masses between 15 and 20.4 mg. Space velocity is defined by

$$SV = \frac{\dot{V}}{m_{cat}}$$

The reactor outlet was maintained at 300 °C to prevent condensation of products. A 7890A gas chromatograph (Agilent) equipped with FID for organic compounds and TCD for total oxidation products CO$_x$.

It was made sure that the catalyst has reached steady state by running the catalyst for at least 12 h or until several GC measurements showed identical results. All measurements were completed back to back. To make sure no deactivation occurred the initial reaction conditions were set and the results compared. Negligible deviations were found for all catalysts.

3 Results and Discussion

3.1 Characterization of Catalysts

Doping of vanadia with potassium resulted in a slight decrease in surface area at low K/V ratios, as shown in Table 1. Increasing the K/V ratio to 1 reduces the surface area to 31 m^2/g. This result can be explained by the formation of potassium titanate phases as reported earlier [14].

The effect of potassium on the structure of surface vanadia was studied via Raman spectroscopy. The vanadium absorption bands of catalyst without potassium in the Raman spectra (in Fig. 2) contains a single band at 1030 cm^{-1} and a broad one at around 830–980 cm^{-1}. These

Table 1 Surface area, composition in weight percent and K/V atomic ratio for all catalysts

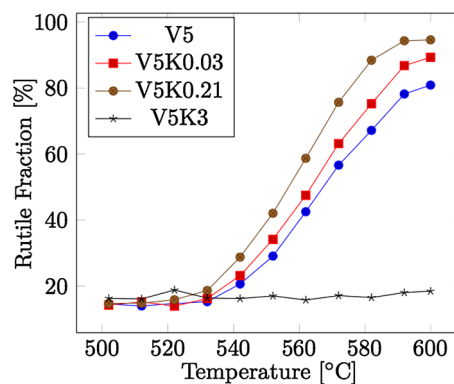| Catalyst	BET surface area [m^2/g]	V$_2$O$_5$ [wt%]	TiO$_2$ [wt%]	K$_2$o [wt%]	K/V atomic ratio
V5	42.6	5.0	95.0	0	0
V5K0.03	38.0	5.0	94.97	0.03	0.01
V5K0.21	38.4	4.4	95.39	0.21	0.1
V5K3.0	31.1	5.0	92.0	3.0	1
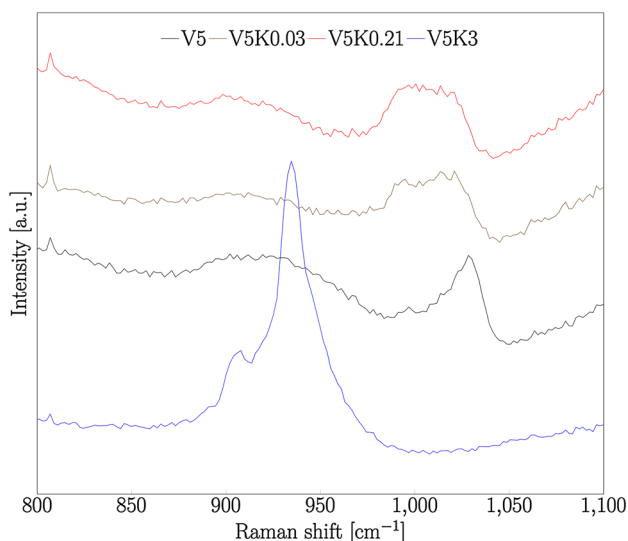
Fig. 2 Raman spectrum of the V_2O_5/TiO_2 catalyst V5 and $K_2O/V_2O_5/TiO_2$ catalysts with different loadings between 800 cm^{-1} and 1100 cm^{-1}

Fig. 3 Rutil fraction of V5 and K promoted catalysts in dependence to temperature

two bands attributed to V=O stretching, correspond to the tetrahedral coordinated vanadate species of monomeric species and to the metavanadate-like polymeric $(VO_x)_n$ species [21].

In the case of catalysts having low potassium content, e.g., in V5K0.03 and V5K0.21, the band at 1030 cm^{-1} (monomeric species) shifts to 1015 cm^{-1} and a new band appears at 995 cm^{-1}. With the presence of potassium, the shift of the high-frequency band indicates a distortion of the monomeric species structure accompanying by the lengthening of the V=O bond [20–22]. This observed perturbation may be interpreted as an electrostatic interaction, like $(Ti–O–)_3V=O^{\delta-}\cdots K^{\delta+}–O$ [22]. Bulushev [22] associated Raman band at 995 cm^{-1} to the K-doped monomeric species, in which part of the bridging Ti–O–V=O sites are substituted by K–O–V=O sites. Upon addition of a high amount of K (K/V = 1), the 1015 cm^{-1} band disappears and a new band at 935 cm^{--1} is detected, which is ascribed to amorphous KVO_3 [23].

The X-ray diffraction patterns confirm that all catalysts contain predominantly anatase up to the calcination temperature of 450 °C. Via in situ high-temperature XRD, the anatase to rutile phase transformation is observed starting at 500 °C and completing at 600 °C. The anatase and rutile relative contents are determined according to the equation reported in literature and shown in Fig. 3 [24].

In this work, formation of rutile for catalyst without potassium is found starting at about 540 °C, which is significantly lower than for pure TiO_2 powder. This is consistent with the well-known promoting effect of vanadia on the anatase to rutile transformation. The phase transformation

is enhanced by the presence of low potassium loading (catalyst V5K0.03 and V5K0.21). The Raman-results show the substitution of Ti^{4+} ions with potassium cations of low valences. Charge neutrality requires an increased presence of oxygen vacancies. Thus, ease of rearrangement and transformation are enhanced by relaxation (lessening of structural rigidity) of the large oxygen sublattice [26]. In the case of catalyst V5K3 with the high potassium loading, no significant change of the rutile fraction is observed and anatase phase is preserved even at 600 °C. This result demonstrates that crystallite KVO_3 hinders the sintering process to higher calcination temperatures.
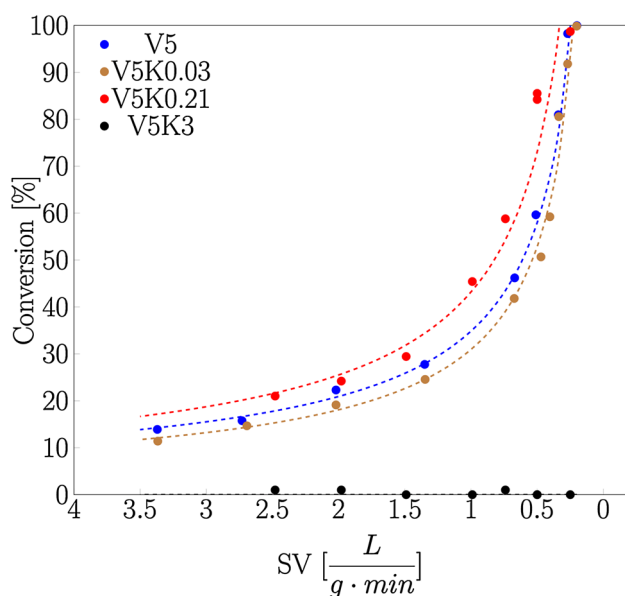
The effect of K-doping on the reducibility of surface vanadia is studied by TPR in hydrogen. The TPR profile of the catalyst without K exhibits two reduction peaks at 406 and 450 °C. These peaks are considered to result from a superposition of different reduction steps of several vanadia species [21]. Doping by 0.03 wt% of potassium results in a significant decrease of the intensity of the first peak at 406 °C and no change in the intensity and position of the second peak at 450 °C as compared to the catalyst V5. The TPR profiles of vanadia in the V5K0.21 catalyst includes several reduction processes with maxima at around 402, 448, 475 and 503 °C (Fig. 4). The increased complexity of the TPR-profile may be attributed to the presence of multitude of potassium-doped surface vanadia species. This result is in line with a variety of vanadia forms found by the Raman spectroscopy. At K/V = 1, the TPR peak at 759 °C can be assigned to the reduction of crystalline KVO_3, as reported in the literature [28]. Vanadia in the catalysts V5K0.21 and V5K3 are reduced noticeably at higher temperatures as compared to the undoped catalyst V5.

3.2 Catalytic Behavior in Oxidation of *o*-Xylene

The changes in conversion of *o*-xylene as a function of the space velocity (SV, L/g*min) are plotted in Fig. 5. For the
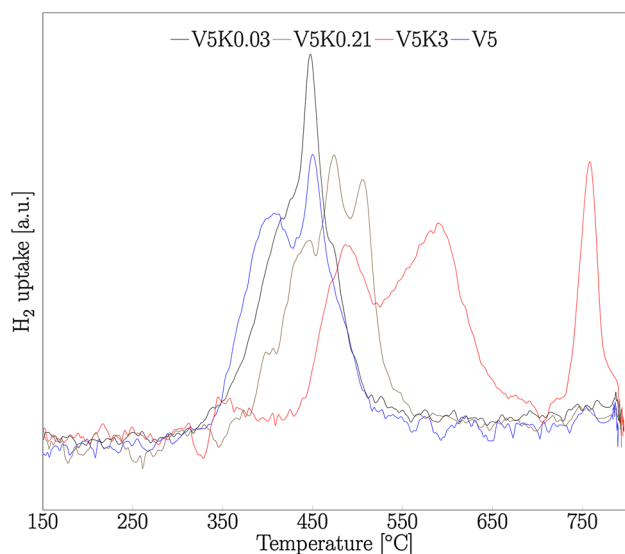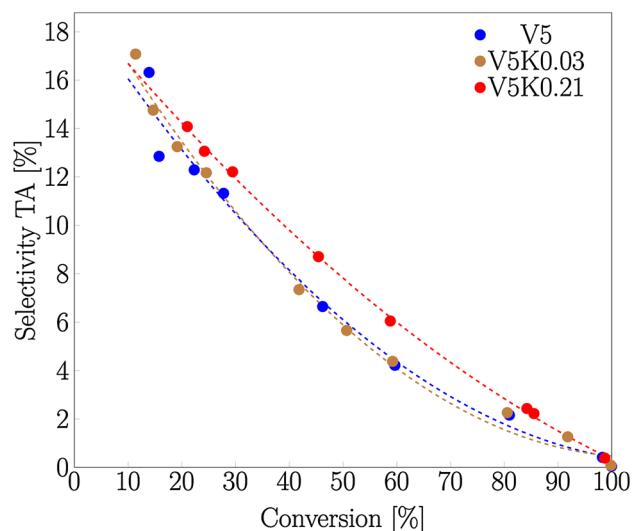
Fig. 4 Hydrogen uptake during a TPR measurement for the V2O5/TiO2 catalyst V5 and K$_2$O/V$_2$O$_5$/TiO$_2$ catalysts with different loadings
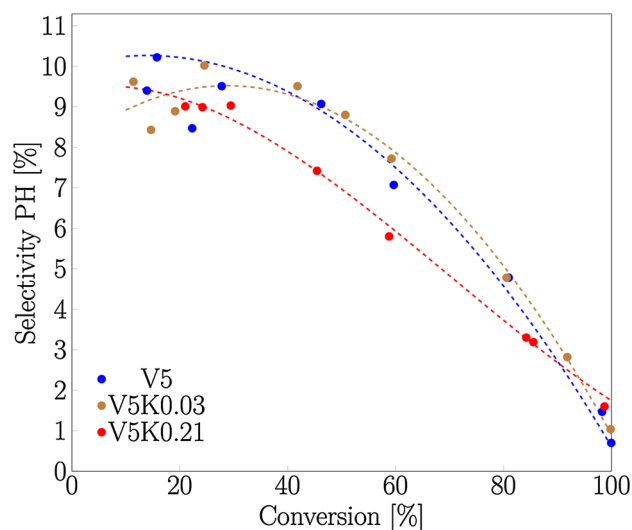

Fig. 6 Selectivity to TA at 350 °C and 1.5 vol% oxylene in air in respect to o-xylene conversion

Fig. 5 O-xylene conversion compared to the weight minutely space velocity at 350 °C and 1.5 vol% oxylene in air

Fig. 7 Selectivity to PH at 350 °C and 1.5 vol% oxylene in air in respect to o-xylene conversion

sample with a loading of 0.03 wt.% potassium, almost no change in activity is observed, being in agreement with TPR results that the maxima of hydrogen consumption for the catalyst V5K0.03 remains unchanged compared to undoped catalyst V5. An increasing amount of potassium results a slight increase in activity, even though the TPR profile shows a shift to higher temperatures. No conversion of *o*-xylene and product formation was found for the catalyst with K/V = 1, containing mainly the crystalline KVO$_3$.

The selectivity patterns for the various products are shown in Figs. 6, 7, 8, 9. For V5K0.03, no difference in the selectivity of TA and for V5K0.21 a slight increase is found, compared to the undoped catalyst V5. Thus, the effect of potassium on the formation of TA is small. Similar to the catalysts V5 and V5K0.03, V5K0.21 shows the PH selectivity of 9% at the conversion up to about 30%. Up to a conversion of ≈30% all catalysts show similar TA selectivites. At higher conversions (>30%), an interesting difference is observed: PH selectivity decreased noticably for V5K0.21. This can be caused by an electro-static interaction between PH and the K doped catalyst surface
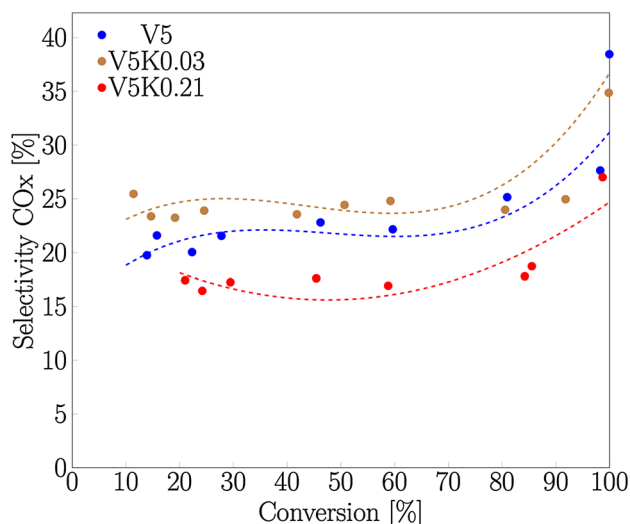
Fig. 8 Selectivity to CO_x at 350 °C and 1.5 vol% oxylene in air in respect to o-xylene conversion
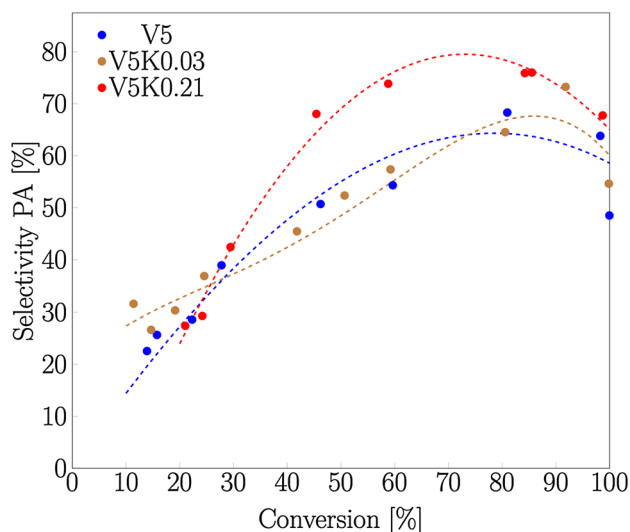
Fig. 9 Selectivity to PA at 350 °C and 1.5 vol% oxylene in air in respect to o-xylene conversion

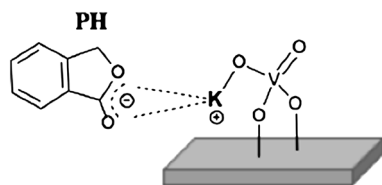**Fig. 10** Possible electrostatic interaction between PH and K

(see Fig. 10). This could facilitate PH adsorption or prevent PH desorption leading to the decrease in PH selectivity. Comparing K doped catalysts with undoped catalyst,

a significant decrease of CO_x selectivity for V5K0.21 and a slight increase for V5K0.03 are seen. It is interesting to observe that the CO_x selectivity for all three catalysts remains nearly unchanged at the conversion up to about 80%. Highest PA selectivity is obtained over the catalyst with the addition of 0.21 wt% K to the V/Ti/O catalyst. These data suggest that the addition of potassium decreases the concentration of electrophilic oxygen species (O_2^-, O^-), responsible for deep oxidation [29], while the concentration of nucleophilic oxygen (O^{2-}), responsible for selective oxidation to PA is increased.

4 Conclusion

Doping of the V/Ti/O catalyst with potassium has an effect on the vanadia surface structure; K-perturbed and K-doped monomeric surface species with an increased length of the V=O bond are formed for small and intermediate loadings. Crystalline KVO_3 are formed with the addition of 3 wt% K. Disappearance of metavanadate-like polymeric species is observed at K/V = 1. In situ high temperature XRD exhibits the influence of potassium on the phase transformation from anantas to rutile. The addition of potassium (0.03 and 0.21 wt%) shows an accelerating effect, while no phase transformation takes place at K/V = 1. TPR in hydrogen provide evidence that K-doped vanadia species are reduced at a higher temperature than the undoped ones. Low addition of potassium (0.03 wt%) shows almost no detectable effect on the catalytic properties of V/Ti/O catalyst. When the catalyst contains an K/V = 1, no catalytic activity is observed, due to the transformation of the monomeric species, responsible for oxidation, into KVO_3 species. Selective oxidation of o-xylene upon K-doping (0.21 wt%) shows a decrease in PH and CO_x selectivity and increase in PA selectivity.

Catalytic data on the selective oxidation of *o*-xylene reveal the influence of potassium on catalytic performance of V/Ti/O catalyst. The addition of potassium provides catalysts characterized by different surface structure and different reducibility of vanadia species. These changes determine the high activity and selectivity in the oxidation of *o*-xylene into phthalic anhydride, for the sample with a loading of 0.21 wt% potassium. With potassium impurities up to 0.03 wt%, almost no influence on the catalytic performance is detected [29, 30].

References

1. Dias CR, Farinha MF, Bond GC (1995) J Catal 157:353

2. Lorz PM, Towae FK, Enke W, Jäckh R, Bhargava N, Hillesheim W (2008) In Ullmann's Encyclopedia of Industrial Chemistry. Wiley, Weinheim

3. Nikolov V, Klissurski D, Anastasov A (1991) Catal Rev 33:319

4. Wainwright MS, Foster NR (1979) Catal Rev Sci Eng 19:211

5. Calderbank PH, Chandrasekharan K, Fumagalli C (1977) Chem Eng Sci 32:1435

6. Creten G, Kopinke FD, Froment GF (1997) Can J Chem Eng 75:882

7. Gimeno MP, Gascón J, Téllez C, Herguido J, Menéndez M (2008) Chem Eng Process, 47:1844.

8. Marx R, Wölk H-J, Mestl G, Turek T (2011) Appl Catal A 398:37

9. Skrzypek J, Grzesik M, Galantowicz M, Solinski J (1985) Chem Eng Sci 40:611

10. Saleh RY, Wachs IE (1987) Appl Catal 31:87

11. Deo G, Wachs IE, Haber J (1994) Crit Rev Surf Chem 4:141

12. Wachs IE, Weckhuysen BM (1997) Appl Catal A 157:67

13. Wachs IE, Saleh RY, Chan SS, Chersich CC (1985) Appl Catal 15:339

14. Bulushev DA, Kiwi-Minsker L, Rainone F, Renken A (2002) J Catal 205:115

15. Wachs IE (1990) J Catal 124 *(2)*:570.

16. BE Handy, I Gorzkowska, J Nickl, A Baiker, M Schraml-Marth, A Wokaun (1992) Ber Bunsenges Phys Chem 96:1832

17. Bond GC, Brückman K (1981) Faraday Disc Chem Soc 72:235

18. SLT Andersson (1986) J Chem Soc Faraday Trans I 82:1537

19. Rodella CB, RWA Franco, Magon CJ, Donoso JP, LAO Nunes, Saeki MJ, Aegerter MA, Sargentelli V, Florentino AO (2002) J Sol-Gel Sci Technol 25:83

20. Deo G, Wachs IE (1994) J Catal 146:335

21. Bulushev DA, Rainone F, Kiwi-Minsker L, Renken A (2001) Langmuir 17:5276

22. Ramis G, Busca G, Bregani F (1993) Catal Lett 18:299

23. Park YS, Shurvell HF J of Raman Spec, 1987, 18:247

24. Spurr RA, Myers H Anal Chem (1957) 29:760

25. Shannon RD, Pask JA J Am Ceram Soc (1965) 48:391

26. KJD Mackenzie Trans J Br Ceram Soc (1975) 74:77

27. Fumagalli C, Golinelli G, Mazzoni G, Messori M, Stefani G, Trifiro F (1993) Cat Lett 21:19

28. Sokolovskii VD (1990) Catal Rev 32:1

29. Bond GC, Zurita JP, Flamerz S, Gellings PJ, Bosch H, van Ommen JG, Kip BJ Appl Catal, **1986**, 22:361

30. van Hengstum AJ, van Ommen JG, Bosch H, Gellings PJ (1983) Appl Catal, 5:207